Autonomous UAV-Assisted IoT Systems with Deep Reinforcement Learning based Data Ferry

Mason Conkel
Electrical and Computer Engr.
University of Texas at San Antonio
San Antonio, Texas, USA
mason.conkel@utsa.edu

Wen Zhang
Electrical and Computer Engineering
Wright State University
Dayton, Ohio, USA
wen.zhang@wright.edu

Mimi Xie
Electrical and Computer Engineering
University of Texas at San Antonio
San Antonio, Texas, USA
mimi.xie@utsa.edu

Yufang Jin
Electrical and Computer Engineering
University of Texas at San Antonio
San Antonio, Texas, USA
yufang.jin@utsa.edu

Chen Pan
Electrical and Computer Engineering
University of Texas at San Antonio
San Antonio, Texas, USA
chen.pan@utsa.edu

***Abstract*—Emerging unmanned aerial vehicle (UAV) technology offers reliable, flexible, and controllable techniques for transferring data collected by wireless internet of things (IoT) devices located in remote areas. However, deploying UAVs faces limitations in mission distance to recharging, especially when recharge occurs far from the monitoring. To address these challenges, we propose smart charging stations installed within the monitoring area equipped with energy-harvest features and communication modules. These stations can replenish the UAV's energy and act as cluster heads by collecting information from IoT devices within their jurisdiction. This allows a UAV to operate continuously by downloading while charging and forwarding the data to the remote server during flight. Despite these improvements, the unpredictable nature of energy-harvest devices and charging needs can lead to stale or obsolete information at cluster heads. The limited communication range may prevent the cluster heads from establishing connections with all nodes in their jurisdiction. To overcome these issues, we proposed an age-of-information-aware data ferry algorithm using deep reinforcement learning to determine the UAV's flight path. The deep reinforcement learning agent, running on cluster heads, utilizes a global state gathered by the UAV to output the location of the next stop, which can be a cluster head or an IoT device. The experiments show that the algorithm can minimize the age of information without diminishing data collection.**

***Index Terms*—UAV, IoT, DRL, Energy Harvesting**

I. Introduction

Recent advances in emerging energy-harvest technologies (EH) [1]–[3], which leverage green energy sources, have demonstrated significant potential for cost reduction, sustainability, and environmental friendliness. These technologies are increasingly seen as vital components of future IoT applications. However, substantial challenges remain in the deployment of EH-powered IoT devices in remote areas, including limited power budgets and line-of-sight (LOS) obstacles, which severely restrict their ability to engage in long-distance communications. Consequently, EH-powered IoT devices often face accessibility issues in such environments, limiting their practical utility and broader deployment.

To address this issue, emerging unmanned aerial vehicles (UAVs) [4]–[8], such as quadcopters, offer reliable, programmable, and diverse methods for data collection and transport across a network. This potential has quickly placed UAVs at the forefront of IoT-related research. However, the deployment of UAVs faces key challenges in the form of flight range due to the limitations imposed by battery capacity.

To combat this, we can strategically place EH-enabled charging stations in operating fields to allow continuous operation and drastically reduce UAV downtime. Using its elevated position in conjunction with long-range communication (LoRa), the UAV offers considerable communication distance at improved reliability compared to fixed infrastructure and provides an avenue for direct communication to remote data servers. However, given the complexity of remote EH-enabled IoT sensor networks, effective communication between these sensors and the UAV remains challenging. Therefore, we will provide charging stations that serve as cluster heads to collect data from sensors under their jurisdictions for transfer to the UAV.

Despite the potential of the proposed solution, limited EH power, extensive monitoring area, and UAV charging can lead to stale or obsolete sensor data. To promote efficiency of communication, this work begins by configuring IoT sensors as semi-passive components that utilize ambient backscatter communication (AmBC) as specified by passive LoRa (PLoRa) [9]–[12]. Cluster heads then collect data while tracking nonresponsive sensors in their jurisdiction. To promote fresh data collection, a deep-reinforcement-learning age-of-information adaptive decision framework (DRL-AoI-ADF) was proposed to take the UAV's knowledge of all cluster heads with the current target's knowledge of its IoT sensors as input and output the next target as a cluster head location or IoT sensor and cluster head location pair to minimize *maximum AoI*. To minimize UAV energy consumption, multiple agents, which share a DRL model structure but provide unique observations, are deployed

978-3-9826741-0-0/DATE25

at each cluster head to decide the upcoming destination. To the best of our knowledge, this is the first work that implements DRL to empower a UAV to perform autonomous data ferrying for IoT networks of EH-powered IoT sensors and cluster heads. In summary, the major contributions of this work are as follows.

1) We propose a sustaining mechanism in the UAV to keep it in the field and eliminate its substantial energy overhead to travel to a remote server to charge.
2) Passive long-range communication is proposed to be integrated into UAV-assisted IoT networks to minimize the energy consumption of IoT devices with improved reliability.
3) We augment a DRL AoI Data Ferry scheme for sensor communication to minimize age of information (AoI).

The remainder of this paper is organized as follows. Section II outlines related research, and Section III explains the motivation behind this work. Sections IV and V propose the system model and the AoI scheme. Section VI presents the experimental results. Section VII concludes this work.

II. Related Work

Energy Efficient IoT: Most related works focus on improving the sustainable IoT network and those technologies that impact the network. [1]–[3] inspire and provide the foundation for the EH features in the network. [3]–[5] provide the foundation for low-power communications while [9]–[12] provide the specific communication type, PLoRa, used in this paper. Finally, [6]–[8] provide a basis for full-network interdependence and optimization. To the best of our knowledge, this paper is the first work to implement DRL for EH-powered networks with direct sensor communication.

UAV Control: Many recent work explored the control of a UAV in an IoT network. [13]–[15] use data freshness or AoI to train reinforcement learning (RL) models with different roles for energy in the network. [16] uses these metrics for DRL training. These works provide a foundation for choosing the model and metrics are deployed to train that model. A major difference from these works is that the UAV can communicate with sensors that do not respond to their cluster heads to ensure network coverage.

III. Motivation

Energy consumption is a major challenge for UAV data transmission. Consider a scenario in which a UAV has a flight time of 45 minutes during which it must travel 1 km between the monitoring area and the charging station, which requires about 8 minutes (round trip) and 20 minutes to recharge. Consequently, under optimal conditions, 37 minutes are available for monitoring, equating to an operational up-time of 57%. Furthermore, the energy overhead associated with commute is at least 17.8%. These figures do not include other overheads or the impact of active communication.

To address the challenge of energy consumption, this paper proposes strategic placement of cluster heads within the monitoring area that provide on-site charging and direct communication support. This will not only minimize downtime, but also enhance UAV operational capabilities. Building upon this environment, this paper also proposes an Adaptive Decision Framework (ADF) augmentation for managing these networks. Despite extensive theoretical research on the management of the Age of Information (AoI) and efficient data collection, there exists a notable gap in applying these concepts to practical energy-harvest scenarios. This work aims to bridge this gap by integrating real energy traces, communication costs, and UAV overhead into a comprehensive framework, thereby facilitating the practical deployment of UAV networks in real-world environments.

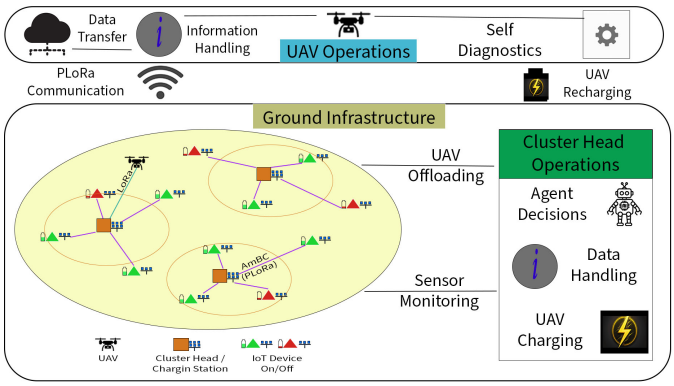

Fig. 1. Proposed UAV-assisted IoT Network

IV. System Model

Fig. 1 illustrates the proposed framework for the remote network made of IoT sensors, cluster heads, and a UAV. This section will discuss how these components are modeled and provide the foundation on which the Adaptive Decision Framework (ADF) is built.

We randomly place M IoT sensors throughout the monitoring area where the location of sensor m is denoted by (x_m, y_m). A K-Means algorithm clusters sensors into N groups such that $N < M$. A cluster head is placed on the centroid of each cluster such that the cluster head n of N is located at (x_n, y_n). The random deployment of sensors simulated a third-party deployment out of sensors out of an engineer's control, while the K-means algorithm provides a simplified process to place cluster heads and determine jurisdiction.

We employ passive long-range communication (PLoRa) [11] between the cluster heads and the UAV. Meanwhile, the carrier wave can power sensor communication using ambient backscattering (AmBC) and allows sensors to relay data by reflecting the data-injected wave. Here, the LoRa wide area network (LoRaWAN) was selected as the carrier wave to enable long-range, low-power and line of sight (LoS) communication up to 5 km for flexible and energy efficient UAV orchestration. In contrast, AmBC in PLoRa has a maximum range of 500 m, and a spreading factor of eight ensures the bit rate and the signal-to-noise ratio (SNR) were nominal.

A. Data Aggregation

Given the optimal transmission rate R_{max} and the average bit error rate $BER_{(comm)}$, the data transmitted D_{trans} during the transmission period t_{trans} can be calculated with Eq. (1).

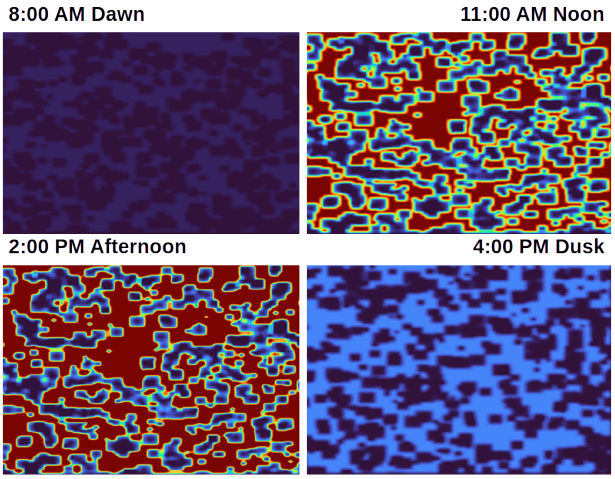

Fig. 2. Power density of area at given times. Scaled from blue (least power) to crimson (most power). Dark regions are attributed to regional features, such as tree coverage.

$$D_{trans} = R_{max} \times (1 - BER_{(comm)}) \times t_{trans} \tag{1}$$

At time step t_{step}, the total data collected by the UAV D_{total} and the total contribution of each cluster head D_n can be calculated by Eq. (3) and Eq. (2), respectively.

$$D_{total} = \sum_{n=1}^{N} D_n(t_{step}) \tag{2}$$

$$D_n = \sum_{t=1}^{t_{step}} D_{trans}(t) \tag{3}$$

The time of last transmission from a cluster head to a sensor t_{packet_m} can be used to extract the cluster head AoI AoI_n in Eq. (4) using the minimum t_{packet_m}. The maximum AoI_{peak}, can be determined using Eq. (5).

$$AoI_n = t_{step} - \min_{m=0 \to M} \; t_{packet_m} \tag{4}$$

$$AoI_{peak} = \max_{\forall n \in R^N} \; AoI_n(t_{step}) \tag{5}$$

B. Energy Model

Each cluster head and sensor is equipped with solar cells. In particular, we refer to PVLib for total solar irradiance (TSI) [17] in our experiments. Next, we obtain power density maps as seen in Fig. 2, by modifying the provided power with a time filter. This time stamp allows for a step size t_{size} equal to one minute. Given TSI, the harvested power $P_{harvest}$ can be estimated with the area A_{cell} and low L and high H wavelengths λ per solar cell using Eq. (6).

$$P_{harvest} = A_{cell} \times \int_{L}^{H} TSI \; d\lambda \tag{6}$$

C. Energy Harvesting

Using $P_{harvest}$, total power of cluster head P_n is determined by communication cost P_c, cost of charging the UAV B_{chg} and the stored reserves P_{batt}. In Eq. (7): c is one channel of total communication channels C_n on cluster head n.

$$P_n = P_{batt} + P_{harvest} - B_{chg} - \sum_{c=1}^{C_n} P_c \tag{7}$$

We define B_{uav} as the maximum battery reserve of the UAV. Given the charging rate R_{chg} of the UAV, the transfer of power from a cluster head to the UAV B_{chg} can be determined over time t_{chg} using Eq. (8).

$$B_{chg} = t_{chg} \times R_{chg}, \qquad B_{chg} \leq B_{UAV} < P_{batt} \tag{8}$$

The battery reserves at the next time step $B_{(t_{step}+1)}$ are determined using current reserves $B_{t_{step}}$ through Eq. (9): c is a channel of total UAV communication channels C_{UAV}.

$$B_{(t_{step}+1)} = B_{t_{step}} + B_{chg} - \sum_{c=1}^{C_{UAV}} P_c \tag{9}$$

V. AoI Minimization for Self-Sustaining Air-Ground IoT System

To minimize AoI, we train and deploy a deep reinforcement learning (DRL) model for intelligent UAV path planning. Given the complex nature of UAV-assisted IoT, this paper improves on the model using Algorithm 1. The supplementary structure ensures robust and adaptable performance.

A. Network Constraints

The constraints placed on the system are as follows.

1) Energy consumption by the IoT network addressed by solar harvesting IoT sensors and cluster heads.
2) Communication specifications accomplished by PLoRa's overhead, range and AmBC.
3) Controlled data freshness through the implementation of AoI monitoring.

B. AoI Minimization

State. State S is represented by an $(N + 6) \times 2$ matrix. The first row s_0 is expressed as $s_0 = [D_{total}, B_{t_{step}}]$. The next N rows are represented by $s_n = [D_n, \; AoI_n] \; | n \in R^N$. The last 5 rows are represented by $s_n = [d_m, AoI_m] \; | m \in R^{M_n}$ where d_m is the distance between the cluster head and the sensor and AoI_m is the AoI of that sensor. We assume that the state varies over time.

Action. In contrast to models that output coordinates, this paper arranges the ADF to return the next cluster head or sensor to target. This reduces the model complexity to output a one-hot encoding. Therefore, the action a taken from the action space A could be defined as $a = n \; | n \in R^{N+5}$.

Reward. Three factors contribute to the reward. The reward for the peak age r_{peak} is evaluated using the current step and AoI_{peak} from Eq. (5) to produce Eq. (10).

Algorithm 1 ADF:Adaptive Decision Framework

Input: $\forall d \in \mathbb{R}^{N+1}$,
$q_{uav}(x_{uav}, y_{uav})$,
$q_n(x_n, y_n),\ D_n,\ AoI_n\ \forall n | n \in \mathbb{R}^N$,
$D_{total},\ B_{t_{step}}$
Output: $n_{target} \in \mathbb{R}^N$

1: **if no** n_{target} **then**
2: $n_{target} = \min_{\forall n \in R^N} d(q_{UAV}, q_n)$
3: **else if** $\forall n \in N\ \exists n\ |AoI_n = 0$ **then**
4: $n_{target} = \{n\ |AoI_n = 0\}$
5: **else**
6: $n_{target} = DDQN(d, D_n, AoI_n, D_{total}, B_{t_{step}})$
7: **end if**
8: **if** $1.2 \times P_{n\_target\_path} \leq B_{uav}$ **then**
9: UAV returns to original n_{target}.
10: **end if**
11: **return** n_{target}

Algorithm 2 Training:ADF Model Training

Input: State S, Action a, Reward r_{final}
Parameters: $Q^A \leftarrow$ **initialize** DQN
$Q^B \leftarrow$ **initialize** DQN
$B_{mem} \leftarrow$ **empty** Deque
$S \leftarrow env(\textbf{reset})$

1: **while** step $\leq$ max_steps **do**
2: $a = Q^A(A)$
$A', r_{finial} \leftarrow env(a|s)$
$B_{mem} \leftarrow \{S, a, S', r_{final}\}$
3: **if** len(B_{mem}) $\geq$ batch_size **then**
4: Update Q^A
5: **end if**
6: **if** step % hard_update_timer = 0 **then**
7: $Q^B \leftarrow Q^A$
8: **end if**
9: $S \leftarrow S'$
10: **end while**

$$r_{peak} = 1 - \frac{AoI_{peak}}{t_{step}} \tag{10}$$

D_{total} from Eq. (2) provides the reward for data r_{total} using the maximum possible data that can be collected in a timestep $D_{max_{step}}$ given by Eq. (11)

$$r_{total} = \frac{\Delta D_{total}}{D_{max_{step}}} \tag{11}$$

Finally, the full reward R is a flat return for crashing or the weighted sum of the other rewards in Eq. (12).

$$R = \begin{cases} -1, & \text{if UAV crashes} \\ \alpha_1 r_{peak} + \alpha_2 r_{total}, & \text{else} \end{cases} \tag{12}$$

C. Adaptive Decision Framework

Using the environmental states, the ADF Algorithm 1 will output a target through the following steps. First, on line 1, ADF ensures that a target n_{target} always exists for the UAV. Next, in line 3, the cluster head checks its state to confirm that every cluster head has been visited before the deep-reinforcement learning (DRL) model makes a prediction. After that, on line 6, the cluster head executes the DRL model to predict the optimal target. Finally, in line 8, the UAV compares the cost of flying to the next target, $P_{n\_target\_path}$ with its current battery level to ensure sufficient energy for flight.

D. ADF Training

Taking the environmental state S, action a and reward r_{final} as inputs, Alg. 2 will drive the decision-making abilities of ADF toward a better reward and performance on the network through the following steps. First, the model is initiated with both deep Q-networks (DQN) and a double-ended queue (deque). At every step, the state and reward are added to the deque in Line 2. When the deque reaches a predetermined batch size, the first DQN is updated in Line 3. Finally, after a set number of steps, the second DQN is updated using the first in line 6.

VI. Experiments

In this section, the experimental environment is introduced including parameter choices and baseline models. Then, the experimental results and implications are discussed.

A. Experimental Setup

The environment is initialized with an area of 1e8 m^2, including a UAV responsible for monitoring 5 cluster heads and 50 sensors as shown in Fig. 3. For the experiment, the assigned numbers correlate to the respective cluster heads.

Each cluster head is equipped with an 800 cm^2 solar panel with a 6.8 Ah maximum capacity battery, while each IoT sensor has an 80 cm^2 solar panel and a 1 F capacitor. The UAV is designed to operate at a maximum speed of 15 m/s, powered by a 6800 mAh battery with a charge rate of 20 minutes and a discharge rate of 45 minutes during flight.

For communication, we use PLoRa described in Section IV, adhering to the reported specifications [11]. The LoRa carrier wave has a maximum range of 5000 m, with an average bit

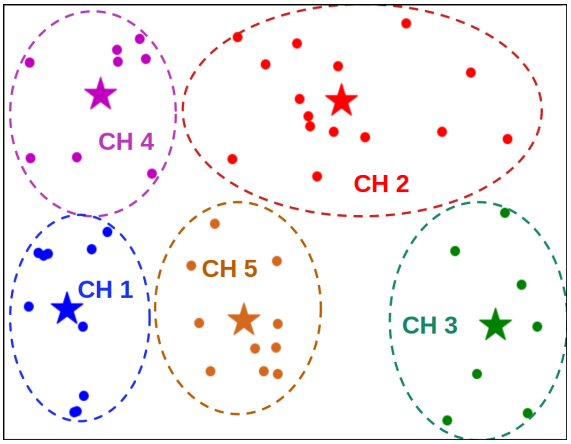

Fig. 3. Network initialization with K-mean clustering.

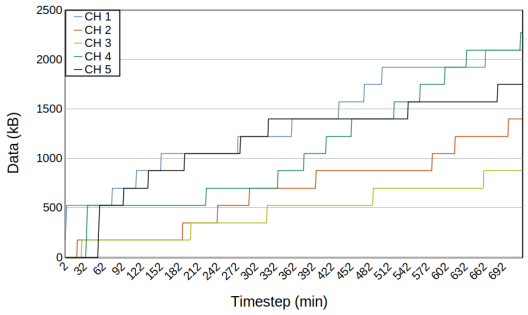

Fig. 4. Time analysis of cluster head data accumulation using DDQN.

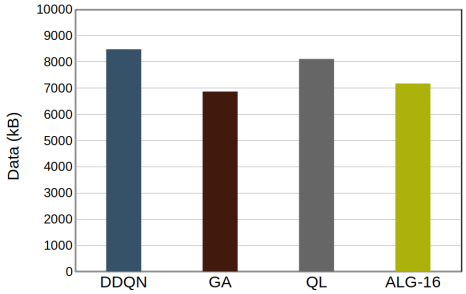

Fig. 5. DDQN data accumulation is comparable to baseline algorithms proving the model does not diminish data collection.

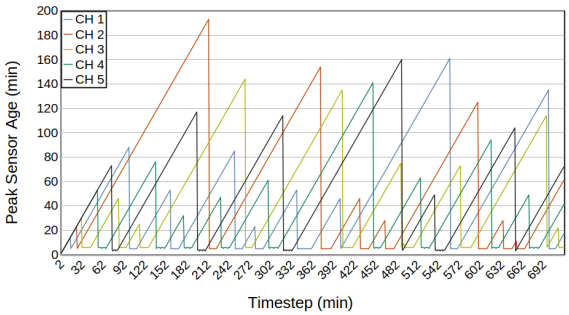

Fig. 6. Time analysis of cluster head AoI_{peak} using DDQN.

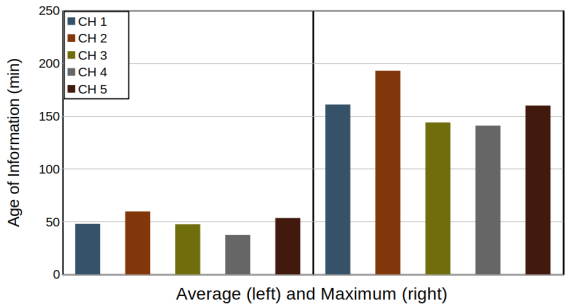

Fig. 7. Comparison of all cluster head AoI_{peak} for DDQN. The left side shows the average peak for each cluster and the right side shows the highest value over the simulation.

error rate (BER) of 0.001 and an optimal transmission rate of approximately 25000 bits per second. The LoRa energy consumption is 4 mW while idle and 20 mW during transmission. In contrast, the ambient backscatter communication (AmBC) in PLoRa supports a maximum range of 500 m, allowing passive communication. This method has a BER of 0.1 and an optimal transmission rate of 1600 bits per second, with an energy cost of 2.6 mW. IoT sensors are configured to collect 300 data samples every 15 seconds, with each sample being 16 bits in size. This data is transmitted to its cluster head on a schedule, transmitting for 30 seconds per IoT sensor.

Each scenario consists of a maximum episode length of 720 steps (equivalent to 12 simulated hours). Initially, we perform 5e4 steps of preoperative training, followed by additional 5e4 steps for full training. These parameters are chosen to optimize data collection, given the transmission rate of AmBC. The chosen DDQN model, consisting of two hidden layers with 128 neurons each, is compared to Q-leaning (QL), Genetic Algorithm (GA) [18], and an algorithm reported in ref. [16] named ALG-16 in the experiments.

B. Experimental Results

The experimental results can be grouped into three categories mentioned in Section IV. Data collection refers to the UAV's ability to accumulate data as mentioned in Section IV-A. AoI refers to AoI_{peak} as mentioned in Section IV-A. Energy refers to energy harvested and spent by the UAV as described in Section IV-C.

Data Collection. One goal of this experiment is to prove that ADF does not jeopardize the total accumulated data. Fig. 4 gives the first indication of the successful performance of ADF. In this figure, the data accumulated by the cluster heads are compared and evaluated over time. DDQN shows adequate data collection with a maximum of approximately 2250 kB from CH 3 and a minimum of 750 kB from CH 4. This displays an offset of 1500 kB that can be attributed to differences in sensor concentration, CH 3 is represented by green in Fig. 3 and contains the fewest IoT sensors.

Fig. 5 provides insight into the total data accumulated compared to the baseline learning models. Here, DDQN shows approximately 500 kB of data accumulation over its machine learning (ML) counterpart, QL. The other models, GA and ALG-16, display a further 1000 kB of data difference, which indicates the successful performance of the DDQN conceptually, as QL also outperforms other baselines, and through comparison of DRL to ML, as it outperforms QL. DDQN performs 6% better than its ML counterpart and 21% better than other baselines, demonstrating its ability to make decisions without a negative impact on data collection.

Age of Information. In Fig. 6, AoI_{peak} of each CH is shown at every step. Here, the UAV shows consistent service, as can be seen in the continued falling peaks throughout the simulation. Furthermore, Fig. 7 displays the average and maximum AoI_{peak} taken from 720 simulation steps. This figure reveals the UAV's efforts to maintain the average for all cluster heads below 60 mins with simulation-wide maximums below 200 mins. This shows the effort of the UAV to manage cluster heads and provides a basis for comparing to the baseline models.

To further illustrate the performance of DRL in ADF, Fig. 8 compares the maximum AoI_{peak} and the average AoI_{peak} over time with respect to DDQN and baseline models, excluding ALG-16 as its AoI must be calculated without IoT sensors. This figure highlights the minimization of AoI_{peak} using DDQN compared to the ML baselines. Fig. 9 further highlights this by

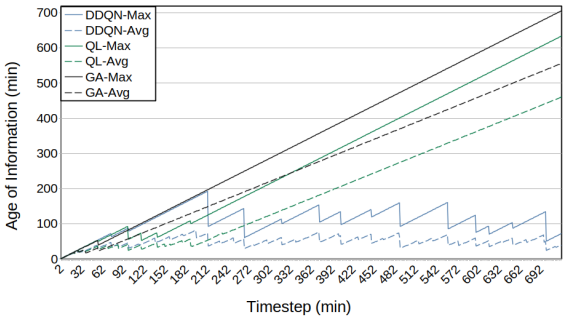

Fig. 8. Comparison of entire network AoI_{peak} metrics over time for DDQN and baseline models. DDQN displays the best control with the light blue curves.

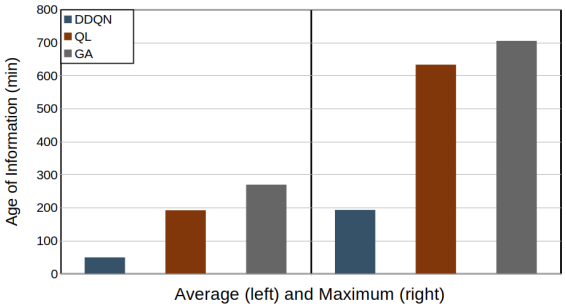

Fig. 9. Comparison of network AoI_{peak} metrics for DDQN and baseline models. The left side shows the average peak for each cluster and the right side shows the highest value over the simulation.

displaying the DDQN's average AoI_{peak} at 26% of the next model and a maximum at 30% of the next.

Table I outlines the standard deviation of DDQN and the baselines. Again, the DDQN displays a lower standard deviation and tighter control of the system compared to the other models. This echoes the usefulness of DRL as the controlling model in contrast to ML counter parts.

Energy. In Fig. 10, the energy spent and harvested by the UAV is shown during DDQN operation. The first marked achievement is the difference between the energy spent on flight, 832 J, and communications, 89 J. With a combined consumption of 921 J, PLoRa only spends approximately 9.7% of the total energy on the UAV. Furthermore, as seen in its linear curve, the UAV can communicate with IoT devices to maintain 100% monitoring, even when recharging.

In terms of energy harvesting, the UAV effectively harvests energy to run continuously over the 12 hour period. The longest period without charging is the initial 40 minutes at which the recharge requirements set by Algorithm 1 on line (8) are met. This explains the discrepancy between the energy consumed (921 J) and the energy harvested (856 J) as that spent from initialization to low battery. The UAV spends less energy on

TABLE I
AoI_{peak} STANDARD DEVIATIONS

	$DDQN$	QL	GA
CH 1	40.4	179.4	7.0
CH 2	51.0	14.2	207.6
CH 3	37.9	196.3	207.0
CH 4	31.0	176.5	206.2
CH 5	38.0	167.5	204.7

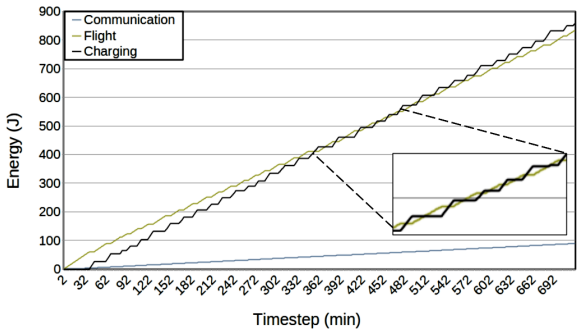

Fig. 10. Time analysis of the accumulated energy spent and harvested by the UAV during the simulation. Communication provides the lowest energy curve in light blue with the flight and charging curves of equal magnitude.

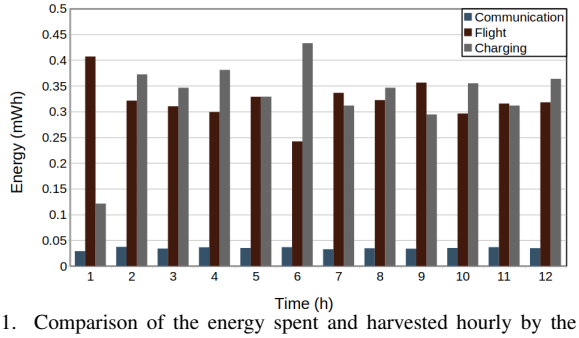

Fig. 11. Comparison of the energy spent and harvested hourly by the UAV during each hour of monitoring.

flight than the energy gained by harvesting, although only charges while docked: shown by the enlargement of Fig. 10.

In Fig. 11, the energy, in mWh, is calculated hourly. It is easier to depict the differences between the energy spent on PLoRa, <0.05 mWh, and on flight, approximately 0.4 mWh. Furthermore, the first hour only shows approximately 0.1 mWh of energy harvest, with the following hour exceeding 0.35 mWh. Following this, the energy harvested only drops below 0.3 mWh in hour 9 of operation. This demonstrates the achievement of low-energy communication and self-sustainability.

Further consideration can be given to the decision made in Alg. 1 in line (8) to allow scheduling charging periods that allow the UAV to further lower the AoI_{peak} of the system and avoid the charging gap shown during the first hour of operation.

VII. Conclusion

This paper develops an age-of-information-aware adaptive decision framework (ADF) to orchestrate a low-power, UAV-assisted self-sustaining IoT network for remote areas. This paper presents the techniques for the simulation of solar cells to power IoT devices, the integration of low-power communications in the form of passive long-range (PLoRa) communications, and the inclusion of active edge devices referred to as cluster heads that can assist a UAV with recharging and IoT sensor monitoring. This paper also formulates ADF and the metrics on which the DRL model is trained. The experimental results demonstrate the performance of the ADF with evidence of its superiority in terms of data accumulation, AoI, and energy consumption by comparing the proposed ADF to baseline counterparts.

REFERENCES

[1] Chen Pan, Mimi Xie, and Jingtong Hu. Maximize energy utilization for ultra-low energy harvesting powered embedded systems. In *2017 IEEE 23rd International Conference on Embedded and Real-Time Computing Systems and Applications (RTCSA)*, pages 1–6. IEEE, 2017.

[2] Chen Pan, Mimi Xie, Song Han, Zhi-Hong Mao, and Jingtong Hu. Modeling and optimization for self-powered non-volatile iot edge devices with ultra-low harvesting power. *ACM Trans. Cyber-Phys. Syst.*, 3(3), August 2019.

[3] Zhenyu Zhou, Chuntian Zhang, Jingwen Wang, Bo Gu, Shahid Mumtaz, Jonathan Rodriguez, and Xiongwen Zhao. Energy-efficient resource allocation for energy harvesting-based cognitive machine-to-machine communications. *IEEE Transactions on Cognitive Communications and Networking*, 5(3):595–607, 2019.

[4] David W Matolak and Ruoyu Sun. Air–ground channel characterization for unmanned aircraft systems—part i: Methods, measurements, and models for over-water settings. *IEEE Transactions on Vehicular Technology*, 66(1):26–44, 2016.

[5] Yong Zeng and Rui Zhang. Energy-efficient uav communication with trajectory optimization. *IEEE Transactions on Wireless Communications*, 16(6):3747–3760, 2017.

[6] Cheng Zhan, Yong Zeng, and Rui Zhang. Energy-efficient data collection in uav enabled wireless sensor network. *IEEE Wireless Communications Letters*, 7(3):328–331, 2017.

[7] Jie Gong, Tsung-Hui Chang, Chao Shen, and Xiang Chen. Aviation time minimization of uav for data collection from energy constrained sensor networks. In *2018 IEEE Wireless Communications and Networking Conference (WCNC)*, pages 1–6. IEEE, 2018.

[8] Wen Zhang, Wenlu Wang, Mehdi Sookhak, and Chen Pan. Joint-optimization of node placement and uav's trajectory for self-sustaining air-ground iot system. In *2022 23rd International Symposium on Quality Electronic Design (ISQED)*, pages 1–6, 2022.

[9] Xiuzhen Guo, Longfei Shangguan, Yuan He, Jia Zhang, Haotian Jiang, Awais Ahmad Siddiqi, and Yunhao Liu. Efficient ambient lora backscatter with on-off keying modulation. *IEEE/ACM Transactions on Networking*, 30(2):641–654, 2022.

[10] Fei Xiao, Wei Kuang, Huixin Dong, and Yiyuan Wang. Backscatter-assisted collision-resilient lora transmission. *Sensors*, 22(12), 2022.

[11] Yao Peng, Longfei Shangguan, Yue Hu, Yujie Qian, Xianshang Lin, Xiaojiang Chen, Dingyi Fang, and Kyle Jamieson. Plora: a passive long-range data network from ambient lora transmissions. In *Proceedings of the 2018 Conference of the ACM Special Interest Group on Data Communication*, SIGCOMM '18, page 147–160, New York, NY, USA, 2018. Association for Computing Machinery.

[12] Naor Zohar. Efficient data gathering from passive wireless sensor networks. In *2021 Wireless Telecommunications Symposium (WTS)*, pages 1–6, 2021.

[13] Zekun Jia, Xiaoqi Qin, Zijing Wang, and Baoling Liu. Age-based path planning and data acquisition in uav-assisted iot networks. In *2019 IEEE International Conference on Communications Workshops (ICC Workshops)*, pages 1–6. IEEE, 2019.

[14] Sarder Fakhrul Abedin, Md Shirajum Munir, Nguyen H Tran, Zhu Han, and Choong Seon Hong. Data freshness and energy-efficient uav navigation optimization: A deep reinforcement learning approach. *IEEE Transactions on Intelligent Transportation Systems*, 2020.

[15] Kun Chen and Longbo Huang. Age-of-information in the presence of error. In *2016 IEEE International Symposium on Information Theory (ISIT)*, pages 2579–2583, 2016.

[16] Mason Conkel, Wen Zhang, and Chen Pan. Enhancing self-sustaining iot systems with autonomous and smart uav data ferry. In *2024 25th International Symposium on Quality Electronic Design (ISQED)*, pages 1–7, 2024.

[17] William F. Holmgren, Clifford W. Hansen, and Mark A. Mikofski. pvlib python: a python package for modeling solar energy systems. *Journal of Open Source Software*, 3(29):884, 2018.

[18] Ahmed Fawzy Gad. Pygad: An intuitive genetic algorithm python library, 2021.